Electronic structure and thermodynamic properties of Fe_2VGa

Andrzej Ślebarski and Jerzy Goraus
Institute of Physics, University of Silesia, 40-007 Katowice, Poland

(Received 28 April 2009; revised manuscript received 26 June 2009; published 16 December 2009)

The aim of this work is to investigate electronic structure, magnetic susceptibility, specific heat, and electrical resistivity of Fe_2VGa and the series of $Fe_2V_{1-x}Ti_xGa$ Heusler alloys. We report x-ray photoelectron valence-band spectra and compare the results with those obtained from full potential linear augmented plane wave method. Fe_2VGa is calculated as nonmagnetic semimetal with a pseudogap located at the Fermi level. Disordered Fe atoms which occupy the V sites, make magnetic clusters, which give rise to negative giant magnetoresistance (GMR). We found that the Kondo coupling between the low density of carrier and the magnetic moments is not sufficient to screen the moments, which form a superparamagnetic state below ~ 20 K. The low temperature decrease in the resistivity and the GMR effect result from a decreased magnetic scattering as the compound orders magnetically. A detailed analysis of the transport and thermodynamic properties reveal a metal-insulator transition in Fe_2VGa, closely resembling that of Mn doped FeSi. The Ti doping increases the density of carriers, in consequence the system for $x>0.2$ is metallic.

DOI: 10.1103/PhysRevB.80.235121 PACS number(s): 71.10.Hf, 71.20.Be, 71.27.+a, 75.20.Hr

I. INTRODUCTION

The metal-insulator (or semiconductor) transitions are continuously studied in various correlated systems,[1] for which the low-T dependences of the macroscopic physical properties characteristic of the Landau theory of Fermi liquids,[2] are observed when $T\rightarrow 0$. Among them there is a class, the so-called *Kondo insulator*, which has a narrow energy gap of the order ~ 10 K at low temperatures. This class of compounds exhibits the Kondo effect at high temperatures and an insulating behavior at low temperatures. Usually, the heavy-electron Fermi liquid (HF) with a large value of the linear specific-heat coefficient, $\gamma \equiv C/T$, is formed in the intermetallic f-electron compounds. FeSi is a nonmagnetic narrow gap semiconductor[3] (or Kondo insulator) with unusual features that it shares with a class of rare-earth compounds known as hybridization gap semiconductors or Kondo insulators.[4] Some other transition-metal-based materials have characteristics similar to those of f-electron HF or Kondo insulator systems. The physics of these d-electron intermetallic compounds with electronic gaps or pseudogaps at the Fermi level are therefore studied extensively. Recently, the Heusler-type Fe_2VAl (Ref. 5) and Fe_2TiSn (Ref. 6) compounds have been discussed as possible d-Kondo insulators of the FeSi-type[7] due to their unusual electric transport and thermodynamic properties. Namely, the electrical resistivity of Fe_2VAl and Fe_2TiSn exhibits semiconducting-like behavior and the low-T specific-heat data revealed an unusual upturn in C/T, commonly observed in heavy fermion systems. The low-temperature specific-heat measurements for $T\rightarrow 0$ yield a term γT with $\gamma \sim 18$ mJ/mol K^2 for Fe_2VAl,[8] and ~ 80 mJ/mol K^2 for Fe_2TiSn,[6] which results in an effective mass about 20 and 40 times as large as bare electron band mass, respectively. This mass enhancement is thought to originate from spin fluctuations[9,10] or from excitonic correlations.[11] Within the tight-binding localized muffin-tin orbital (TB-LMTO) approximation,[12] electronic structure calculations indicated that Fe_2TiSn and Fe_2VAl should be a nonmagnetic semimetal with a pseudogap in the density of states (DOS) at the Fermi level. In this regard, both alloys show an apparent similarity to a nonmagnetic narrow-gap semiconductor, FeSi, which has been classified as a unique d-electron Kondo insulator. However, when the specific-heat measurements were carried out in the magnetic fields, they showed, that the upturn in $C(T)/T$ was rather due to a Schottky anomaly arising from magnetic clusters, but not to Kondo interaction.[8] Also, the band-structure calculations did not give evidence for HF behavior in Fe_2VAl (Ref. 13) and yield only a minor mass renormalization.[9–11,14] Likewise, an infrared (IR) study did not show clear features of the HF state in the electrodynamic response of Fe_2VAl.[15] For Fe_2TiSn IR study suggests that the apparent mass enhancement $\sim 40m_e$, where m_e is the free-electron mass at low temperature is rather due to a Schottky-like anomaly arising from magnetic clusters.[16]

It is well known that the properties of strongly correlated electron system are extraordinarily sensitive to the crystallographic disorder.[17] The electronic structure of Fe_2VAl and Fe_2TiSn is therefore strongly perturbed by antisite disorder near the Fermi level ϵ_F. Deniszczyk and Borgieł have shown,[18,19] using TB-LMTO numerical calculations, that the Fe antisite defects in the nonmagnetic Fe_2VAl and Fe_2TiSn give rise to the narrow, strongly correlated d-like band located just below the Fermi level in the pseudogap. Taking into account the analysis of the one-particle electronic structure, they showed that the many-body investigations qualitatively follow the experimental $\rho(T)$ and $C(T)/T$ observations. The character of the ground-state behavior in these d-electron correlated materials has, however, not been solved yet.

Electronic structure calculations within the full-potential screened Korringa-Kohn-Rostocker (FSKKR) method indicated that Heusler alloys show a Slater-Pauling behavior and the total spin-magnetic moment per unit cell scales with the total number of valence electrons following the rule $M=Z-24$.[20] Basing on the results obtained in Ref. 20, Fe_2VGa (also Fe_2VAl and Fe_2TiSn) should be a nonmagnetic semimetal, with a pseudogap in the DOS at the Fermi level. Indeed, Fe_2VGa was predicted from band-structure calcula-

tions to be semimetallic and nonmagnetic.[21] The NMR measurements[22] also supported the assignment of Fe_2VGa as a band semimetal with a finite DOS at the Fermi level. Resistivity $\rho(T)$ data, however, did not display activated behavior[23] at the low temperatures and supported the metallic (semimetallic) character of Fe_2VGa. Fe_2VGa is also known as a weak and inhomogeneous ferromagnet. The magnetic properties of this alloy are due to atomic disorder and local off-stoichiometry, characteristic for similar Fe-Heusler alloys discussed above. Anomalous giant magnetoresistance (GMR) effect near 50% reported for Fe_2VGa was a fascinating discovery, which has indicated another possible mechanism which is responsible either for the specific-heat anomaly or the metal-insulator transition.[24] The origin of GMR and other anomalies can be explain qualitatively from the combination of the semiconducting-like matrix and the magnetic clusters formed by antisite magnetic Fe defects and the local environment. There is a large number of the doped magnetic semiconductor,[25] e.g., $Ga_{1-x}Mn_xAs$ with the presence of strong disorder, which plays an essential role in both magnetic and transport properties of the system with the localization of carriers. The doped semiconductor/semimetal Fe_2VGa recently attracts a great deal of attention for the possible applications and the reach physical properties.

The aim of this work is to investigate the electronic structure, electrical resistivity, and magnetic properties of Fe_2VGa. The band-structure calculations predict a semimetallic and nonmagnetic ground state; however, atomic disorder leads to appearance of a magnetic clusters. A set of experiments has been embarked on to elucidate the critical behavior and the role of localized magnetic moments on the both sides of the metal-insulator transition in Fe_2VGa. Our data suggest that Fe_2VGa shows an undercompensated Kondo effect due to the low carrier concentration at the Fermi level. The effect of Ti doping leads to increasing of the density of carriers, in effect the $Fe_2V_{1-x}Ti_xGa$ alloys are well Kondo screened metals for $x>0.2$.

II. EXPERIMENTAL DETAILS

Polycrystalline samples of $Fe_2V_{1-x}Ti_xGa$ have been prepared by arc melting the constituent elements (Fe 99.99%, V 99.99%, Ti 99.99%, and Ga 99.99% in purity) on a water cooled copper hearth in a high purity argon atmosphere with an Al getter. Each sample was remelted several times to promote homogeneity and annealed at 600 °C for two weeks than at 400 °C for 24 hours followed by furnace cooling. The samples were carefully examined by x-ray diffraction analysis and found to be single-phase $L2_1$ Heusler-type structure for $x \leq 0.4$.

The dc magnetization was measured using a commercial superconducting quantum interference device magnetometer (MPMS) from 1.8 to 400 K in magnetic fields of up to 7 T.

Electrical resistivity measurements were made using a standard four-wire technique. The specific heat was measured in the temperature range of 1.8–300 K and in external magnetic fields of 0 and 4 T using a Quantum Design PPMS platform.

The x-ray photoelectron spectroscopy (XPS) spectra were obtained with monochromatized Al $K\alpha$ radiation at room temperature using a PHI 5700 ESCA spectrometer. The spectra were measured immediately after cleaving the sample in a vacuum of 10^{-10} Torr. The spectrometer was calibrated according to Ref. 26. Binding energies were referenced to the Fermi level ($\epsilon_F=0$).

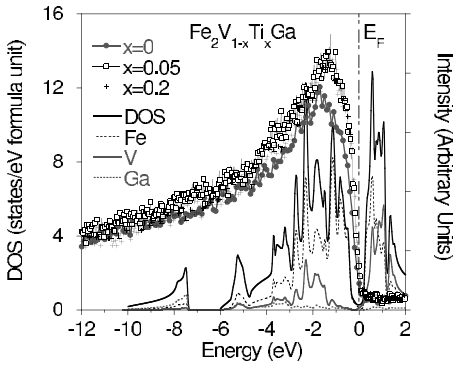

FIG. 1. The total DOS calculated for Fe_2VGa with the use of spin-polarized FP-LAPW approach. The partial densities of states of Fe, V, and Ga are also shown. The total DOS are compared to the measured valence-band XPS data obtained for Fe_2VGa, $Fe_2V_{0.95}Ti_{0.05}Ga$, and $Fe_2V_{0.8}Ti_{0.2}Ga$.

III. COMPUTATIONAL METHODS

We performed the band-structure calculations using WIEN2K full potential linear augmented plane wave (FP-LAPW) code[27] for the experimental lattice parameters. The numerical calculations of the electronic density of states of stoichiometric Fe_2VGa with antisite (AS) defects were performed for $[Fe_{14}V_2^{AS}][V_6Fe_2^{AS}]Ga_8$ unit cell, where two Fe atoms occupied the V positions and vice versa ($Fe_{AS} \leftrightarrow V_{AS}$), assuming a P1 space group of the $2\times1\times1$ supercell.

In order to investigate the influence of Ti on magnetic structure we used a $2\times1\times1$ Pmm2 supercell where 1, 2, 3, or 4 V atoms were replaced by Ti, that correspond to the $Fe_2V_{0.125}Ti_{0.875}Ga$, $Fe_2V_{0.25}Ti_{0.75}Ga$, $Fe_2V_{0.325}Ti_{0.625}Ga$, and $Fe_2V_{0.5}Ti_{0.5}Ga$ compositions. In supercell calculations we used 162 k points in the irreducible Brillouine zone, whereas the FP-LAPW calculations of Fe_2VGa were performed for 560 k points. Calculations were also thoroughly checked for convergence with respect to k point number. The muffin-tin (MT) spheres were 2.34 a.u. for transition elements (Fe,V,Ti) and 2.2 a.u. for Ga. In all case the PBE GGA96 exchange-correlation (XC) potential was used.[28]

IV. RESULTS AND DISCUSSION

A. Electronic structure

In Fig. 1 we show the calculated total and partial atomic DOSs obtained for the stoichiometric and ordered compound Fe_2VGa. Also shown in the figure, for comparison, are the XPS valence-band spectra for Fe_2VGa and $Fe_2V_{1-x}Ti_xGa$ with $x=0.05$ and 0.2. In general, there is a qualitative agreement between the XPS spectra obtained experimentally and the calculated DOS. In Fig. 1 the total DOS spectrum decomposes into two clearly separated parts. A band located in

the binding-energy range of 7.5–10 eV originating mainly from the *s* states of Ga is separated by a gap of ~1.5 eV from the valence band. The upper part of valence band, where the maximum in the DOS occurs, is mainly composed of Fe *d* states. Fe_2VGa appears semimetallic and nonmagnetic in FP-LAPW with the DOS at the Fermi level of ~0.3 eV^{-1} f.u.$^{-1}$. To better understand the properties of real Fe_2VGa crystals, exhibiting strong atomic disorder, we also investigated the electronic structure of Fe_2VGa alloy with one Fe atom occupying the V site. It is well documented[29,30] that in the disordered Fe_2VAl the Fe and V atoms at the antisite positions (Fe↔V) give rise to narrow impurity *d*-band located just in the middle of quasigap calculated for an ordered Fe_2VAl compound.[31] An atomic disorder leads to very similar *d*-band effect in Fe_2TiSn.[19] Recently, we also have shown that this narrow *d*-band formed by the antisite Fe atoms significantly changes the shape of the XPS spectra near the Fermi level.[19]

Results of our FP-LAPW band-structure calculations for defected $[Fe_{14}V_2^{AS}][V_6Fe_2^{AS}]Ga_8$ structure are presented in Fig. 2. The total DOS [Fig. 2(a)] has a pseudogap located ~0.2 eV above the Fermi level and a sharp and narrow *d*-electron peak in the DOS just at ϵ_F. The DOS of this peak is composed mainly of the antisite Fe_{AS} *d* states of iron defects occupying the V sites [in Fig. 2(c)]. In panel (b) we present the calculated DOS for Fe atoms occupying the normal positions. In our calculations the disordered Fe_2VGa is nonmagnetic. Our supercell calculations give no evidence for the formation of magnetic clusters for $[Fe_{14}V_2^{AS}][V_6Fe_2^{AS}]Ga_8$ due to Fe↔V change, but the magnetic AS defects are calculated for larger occupation of V sites by Fe atoms.

In Fig. 3 are presented the XPS valence-band spectra of Fe_2VGa corrected for background[32] and the calculated XPS spectra curves for Fe_2VGa [ordered, (a)] and $[Fe_{14}V_2^{AS}][V_6Fe_2^{AS}]Ga_8$ [disordered, (b)], for which the calculated partial densities of states were convoluted with Lorentzian with a 0.4 eV half-width to account for the instrumental resolution and multiplied by the corresponding cross sections for partial states of Fe, V, and Ga with different *l* symmetry, taken from Ref. 33. The energy spectra of the electrons were analyzed with an energy resolution better than 0.4 eV. In general, there is a qualitative agreement between the XPS spectra obtained experimentally and the calculated ones. However, the high-resolution XPS valence bands clearly show a feature attributed to an antisite Fe contribution in binding energies between ϵ_F and 1 eV. In the near vicinity of the Fermi level (see Fig. 3) the agreement between the measured XPS spectra and calculated one for the disordered Fe_2VGa is very good, which evidently signals the location of the AS *d* states at the Fermi level. At higher binding energies the physical origin of discrepancy between the calculated and measured XPS spectra [either (a) or (b)] is not clear. It can also be attributed to the atomic disorder. Another reason could be a modeling character of background subtraction. In Fig. 3 the XPS spectra obtained experimentally are subtracted in by the backgrounds which have been calculated with approximate (although well validated) Tougaard algorithms.[32]

Figure 4 shows an evolution of FP-LAPW DOS in surrounding of ϵ_F in the series of the $Fe_2V_{1-x}Ti_xGa$ alloys vs

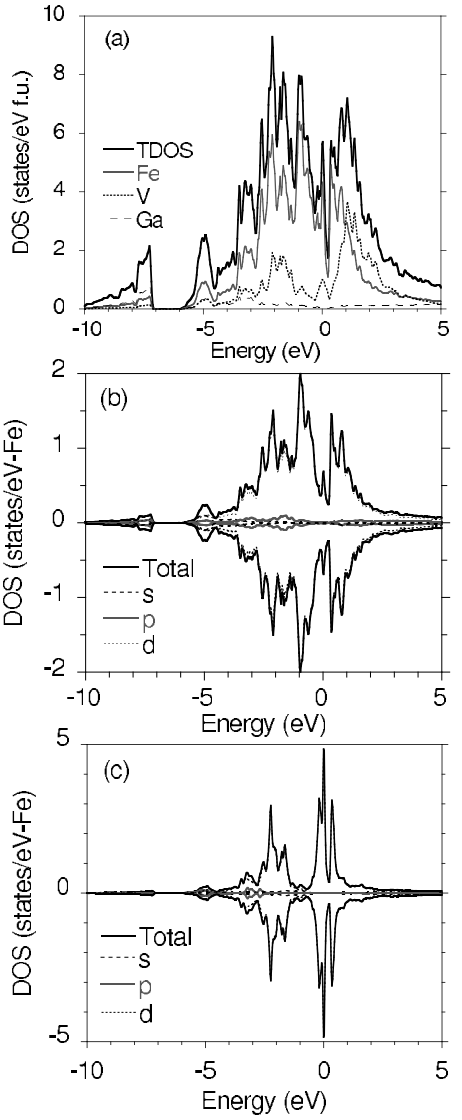

FIG. 2. (a) The total DOS calculated by FP-LAPW *supercell* approach for $[Fe_{14}V_2^{AS}][V_6Fe_2^{AS}]Ga_8$; the partial DOSs are also presented. (b) The calculated DOSs (per one Fe atom) for Fe atoms occupying the normal positions (1–14) in $[Fe_{14}V_2^{AS}][V_6Fe_2^{AS}]Ga_8$. (c) The AS iron *d* states in $[Fe_{14}V_2^{AS}][V_6Fe_2^{AS}]Ga_8$ supercell, occupying the V sites.

concentration of Ti. The doping of Fe_2VGa by Ti decreases the number of valence electrons in the $Fe_2V_{1-x}Ti_xGa$ series. The pseudogaps are located above the Fermi level at $E > \epsilon_F$. With decreasing the number of valence electrons the $Fe_2V_{1-x}Ti_xGa$ alloys are calculated as nonmagnetic for $x = 0.125$ and $x = 0.25$, while the components $x > 0.25$ of the system are magnetic. In consequence, it also appears that all Fe atoms in Fe_2VGa are nonmagnetic with the same DOS in both spin directions. Upon Ti doping a minority density of states dominate the band structure of Fe atoms at the Fermi surface when $x > 0.25$, which leads to the formation of the magnetic moment. The observed in the figure change in DOS vs *x* suggests the following explanation for the onset of magnetism in the series of $Fe_2V_{1-x}Ti_xGa$ alloys. The increasing content of Ti changes the number of *d*-type electrons. For the components of the $Fe_2V_{1-x}Ti_xGa$ series rich in V ($x \leq 0.25$),

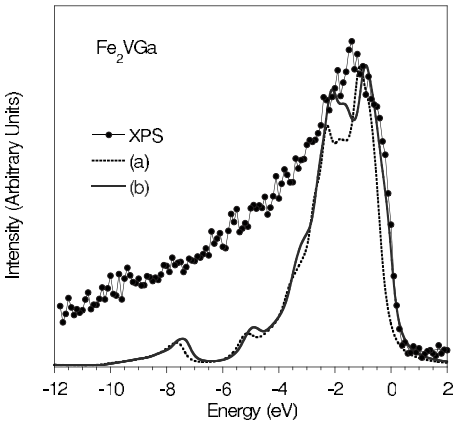

FIG. 3. Experimental valence-band spectrum (corrected by background) compared with the results of the FP LAPW calculations performed for the compound Fe_2VGa (a) and for the $[Fe_{14}V_2^{AS}][V_6Fe_2^{AS}]Ga_8$ supercell (b) containing Fe-AS defects.

the small decrease in the number of $3d$ electrons (less than 20%) causes the distinct shift of the Fermi level toward the top of the valence band. In consequence, the DOS at ϵ_F increases gradually, however, not enough to fulfil the Stoner criterion for magnetic order. The DOSs at ϵ_F satisfy the

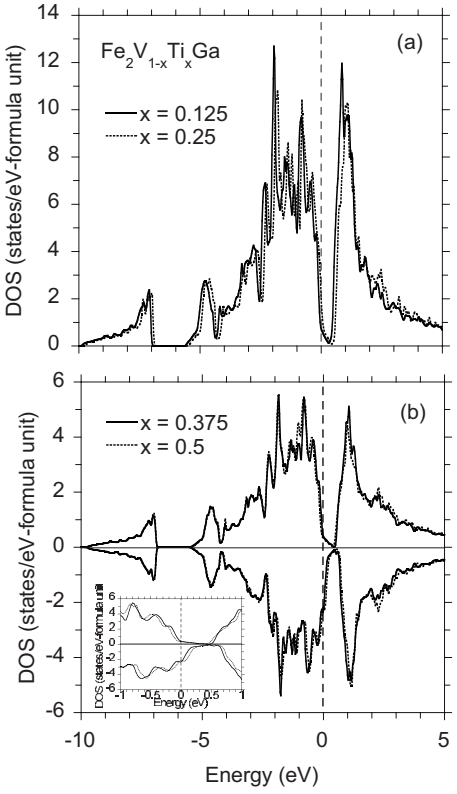

FIG. 4. (a) The total DOS calculated by FP LAPW supercell approach for $Fe_2V_{0.875}Ti_{0.125}Ga$ and $Fe_2V_{0.75}Ti_{0.25}Ga$. In panel (b) the spin-resolved DOS for $Fe_2V_{0.875}Ti_{0.125}Ga$ and $Fe_2V_{0.5}Ti_{0.5}Ga$. The inset shows details near the Fermi level. With increasing x the majority spin bands shifts toward the higher binding energy, giving a pseudogap at ϵ_F. The minority spin bands shifts in the opposite direction towards energies $E > \epsilon_F$. In result, half-metallic-like character of the bands is possible.

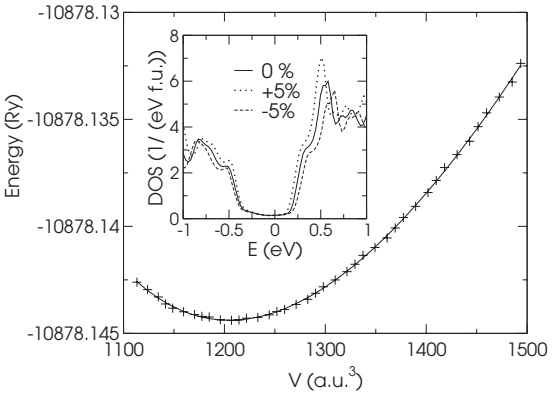

FIG. 5. The energy for several hypothetical Fe_2VGa crystals vs volume 5% on either side of the experimental volume. In the inset are the DOSs near the Fermi level of Fe_2VGa, calculated for volume obtained experimentally and for two hypothetical alloys with the volume 5% larger or smaller.

Stoner criterion for $x > 0.25$ and the components of the $Fe_2V_{1-x}Ti_xGa$ system with the concentration of Ti larger than $\sim 25\%$ become magnetic.

In order to see the effect of external pressure on the pseudo band gap in Fe_2VGa, we calculated the energy for 41 crystal volumes within a $\pm 5\%$ value on either side of the experimental volume. We found that the $\pm 5\%$ change in volume practically does not change the pseudogap (see the inset of Fig. 5). Similar results were obtained for Fe_2VAl.[11] Hence we predict that the effect of lattice pressure resulting from the partial replacement of V by Ti would not change drastically the semimetallic state in $Fe_2V_{1-x}Ti_xGa$. Fit of the second-order Murnaghan equation[34] in Fig. 5 gives the very low value of the bulk modulus $B = 6.8$ GPa, much smaller than that (49 GPa) reported for Fe_2VAl, which indicates a soft lattice.[11] The equilibrium volume $V_0 = 1204.9$ a.u.^{3} gives lattice parameter 5.63 Å, which is 2.2% smaller than the value measured at the room temperature. The change in the number of conduction electrons should be therefore much more important effect in the electric transport properties of the system of $Fe_2V_{1-x}Ti_xGa$ alloys with small x value ($x < \sim 0.1$) then the influence of external pressure caused by doping.

B. Magnetic susceptibility

Shown in Fig. 6 are real (χ') and imaginary (χ'') components of magnetic ac susceptibility χ data plotted as χ' and χ'' vs T between 1.8 and 60 K for (a) Fe_2VGa and (b) $Fe_2V_{0.95}Ti_{0.05}Ga$ alloys. χ' deviates markedly from a Curie-Weiss law and increases when $T \rightarrow 300$ K. This behavior signals spin fluctuations. An alternative suggestion is based on a model that requires the existence of correlated magnetic excited states lying above the nonmagnetic ground state.[3] Figs. 6(a) and 6(b) display the χ' and χ'' frequency dependence, with the maximum reduced with increasing frequency. This is characteristic behavior of spin glasses. The magnetization data presented in Fig. 7 suggest, however, superparamagnetic behavior for Fe_2VGa. We found that for $2 < T \leq 25$ K, M is universal function of H/T. In this tempera-

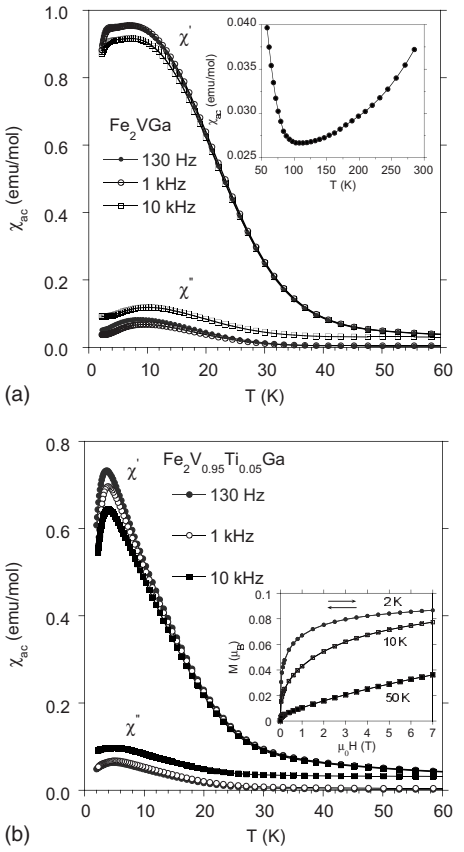

FIG. 6. Real χ' and imaginary χ'' components of ac magnetic susceptibility vs temperature for Fe_2VGa (a) and $Fe_2V_{0.95}Ti_{0.05}Ga$ (b). The inset in panel (a) shows χ' measured at higher temperatures (ν=130 Hz). The inset in panel (b) displays the magnetization vs magnetic field at different temperatures. The saturation magnetic moment μ_S, obtained from an extrapolation of an M vs $1/H \rightarrow 0$, is 0.12 μ_B for Fe_2VGa and 0.09 μ_B for $Fe_2V_{0.95}Ti_{0.05}Ga$.

ture region the magnetization does not show any hysteresis loops in the field dependence of magnetization M. These two experimental features characterize superparamagnetism,[35] therefore the behavior observed here is of the superparamagnetic type rather than the spin glass-type. In Fig. 7 the M vs H data displays, however, a small hysteresis of 22 mT at T =2 K, which suggests the blocking temperature ~2 K [also χ' shows a small maximum at ~2 K, see Fig. 6(a)]. The Arrott analysis in Fig. 7(c) shows that Fe_2VGa is magnetically inhomogeneous and the magnetic clusters are forming without global ordering below ~20 K. A similar superparamagnetic behavior was also found for a doped Fe_2VGa [see Fig. 6(b)].

The important point here for understanding the electrical transport properties and specific heat is the density of magnetic moments, which are created by disorder. Assuming that the Fe antisites dominate in Fe_2VGa and taking g=1.93 and S=3/2 for these defects, the saturation magnetization of Fe_2VGa expressed by $M_S = N_{Fe} g \mu_B S$ gives an impurity concentration of $\sim 1.1 \times 10^{18}$ cm^{-3}. This value of N_{Fe} is comparable to the number of carriers found in similar Heusler alloys: Fe_2TiSn (Ref. 16) or Fe_2VAl.[13] The absolute value of the Drude plasma frequency ω_p implies a carrier density as

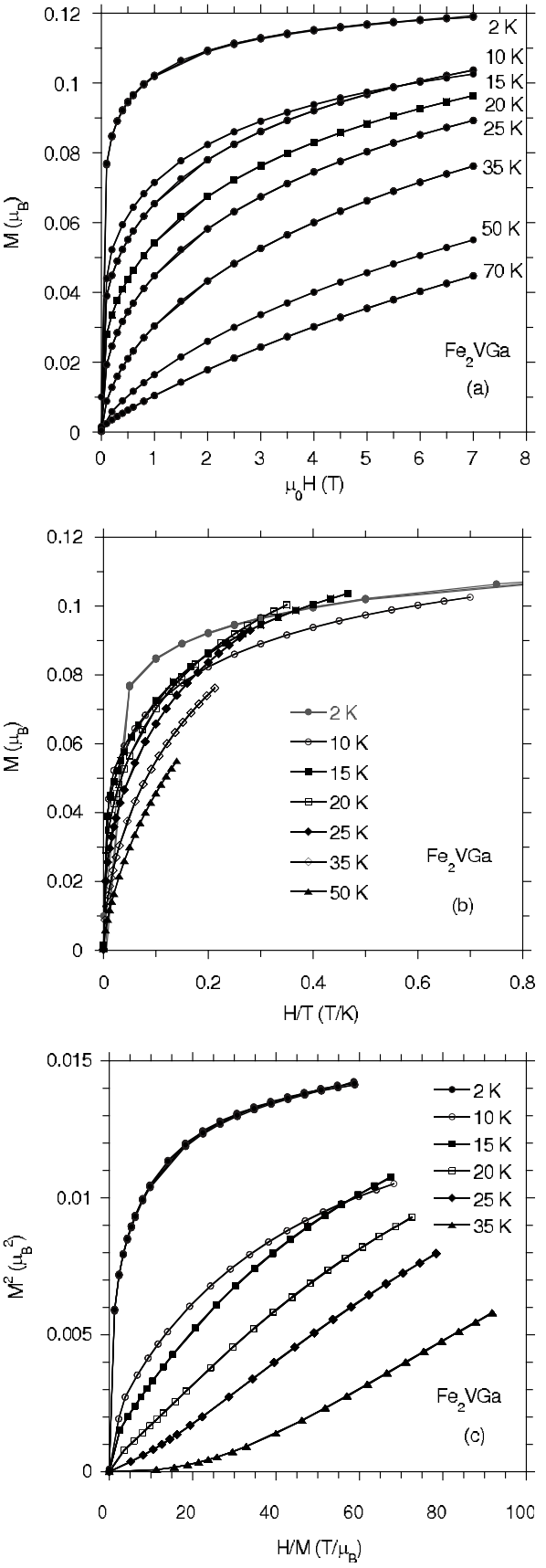

FIG. 7. Fe_2VGa: (a) dc magnetization versus magnetic field H. In panel (b) is shown magnetization M versus H/T, panel (c) displays the M^2 versus H/M.

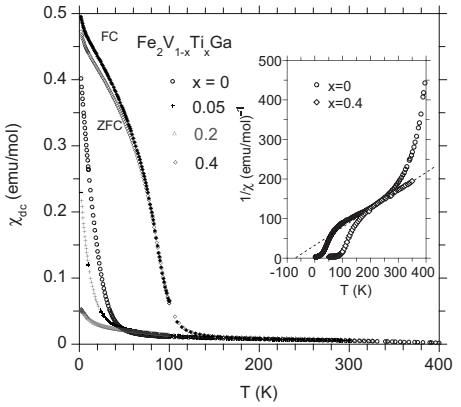

FIG. 8. The ZFC and FC dc susceptibility for $Fe_2V_{1-x}Ti_xGa$.

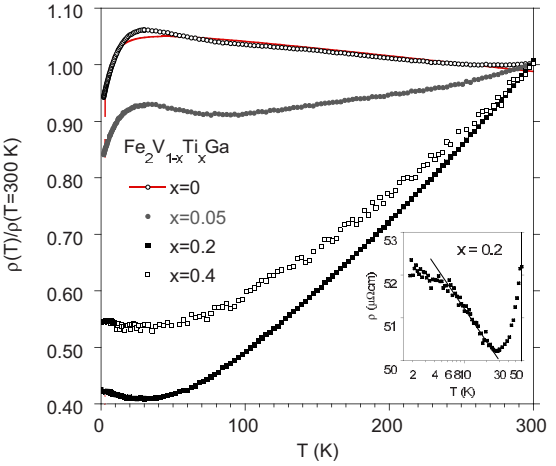

FIG. 9. (Color online) The temperature dependence of the electrical resistivity $\rho(T)$ normalized to the $\rho(T=300\ \mathrm{K})$ for various $Fe_2V_{1-x}Ti_xGa$ samples. The resistivity ρ at 300 K is 415 $\mu\Omega$ cm for Fe_2VGa and 135 $\mu\Omega$ cm for $Fe_2V_{0.05}Ti_{0.05}Ga$. For $x>0.05$ ρ is $\sim$120 $\mu\Omega$ cm at the room temperature. The resistivity of Fe_2VGa obeys the relationship $\rho(T)=a-bT-c/T+e^{\Delta/T}$. The inset displays $\rho(T)$ vs ln T for $Fe_2V_{0.8}Ti_{0.2}Ga$.

small as $n\sim 5\times 10^{20}$ cm^{-3} for Fe_2TiSn, under assumption $m^{\star}=m_0$

In Fig. 8 we summarize the zero-field cooling (ZFC) and field cooling (FC) dc susceptibility for $Fe_2V_{1-x}Ti_xGa$, when $x\leq 0.4$. For the samples $x\leq 0.2$ the magnetic susceptibility deviates markedly from a Curie-Weiss law and has a strong dependence on the concentration x. The plots of χ vs T (and χ^{-1} vs T) for Fe_2VGa, $Fe_2V_{0.95}Ti_{0.05}Ga$, and $Fe_2V_{0.8}Ti_{0.2}Ga$ in Fig. 8 signal the onset of the weak magnetic behavior due to AS Fe defects, with characteristic features in $\chi(T)$ similar to those in χ vs T plot for disordered Fe_2TiSn. The dc magnetic susceptibility of $Fe_2V_{0.6}Ti_{0.4}Ga$ exhibits different behavior. It is hysteretic under ZFC and FC below $\sim$100 K which is typical for inhomogeneous ferromagnets, whereas for $T>200$ K χ obeys the Curie-Weiss law. The paramagnetic Curie-Weiss temperature $\theta\approx -70$ K with the $C=N\mu^2/(3k_B)$ value that is close to the value $C=1.9$ emu K/mol expected for an iron configuration d^7 Fe$^+$. The negative paramagnetic Curie-Weiss temperature suggests the presence of Kondo-type interactions. From the value of θ the Kondo temperature $T_K\sim\theta/4$ may be about 20 K.[36] There is also a small hysteresis at $T=2$ K in the field dependence of the magnetization M, whereas magnetization does not show any hysteresis loops at $T>2$ K such as for samples $x\leq 0.2$. In the case of $Fe_2V_{0.6}Ti_{0.4}Ga$, however, the ferromagnetic particles can contain either the AS magnetic Fe atoms or the remaining Fe atoms occupying all Fe atomic positions, which are magnetic too. The FP-LAPW calculations for $Fe_2V_{0.625}Ti_{0.375}Ga$ predicted a magnetic ground state with a magnetic moment of 0.24 μ_B per formula unit which is comparable to the saturation magnetic moment of $Fe_2V_{0.6}Ti_{0.4}Ga$, $\mu_S=0.14$ μ_B (obtained from an extrapolation of the M vs $1/H$ plots to $1/H=0$). The magnetic ground-state properties of $Fe_2V_{0.6}Ti_{0.4}Ga$ are well explained on the base of Galanakis *et al.*[20] diagram due to the change (decreasing) in valence electrons in the doped Fe_2VGa.

The finite carrier concentration of the doped Fe_2VGa semimetal is the consequence of the Fe-AS impurity band that develops in the gap. Each impurity breaks the translational invariance of the lattice and gives rise to a bound state in the pseudogap (see Fig. 2). For low x ($x<0.2$) the bound states are isolated and localized. The conclusion from magnetic measurements is that there are residual unscreened spins in Fe_2VGa and $Fe_2V_{1-x}Ti_xGa$; $x<0.2$. We are dealing with an undercompensated Kondo problem where there are not enough free carriers with spin $S=1/2$ to screen the remaining local moments associated with AS Fe defects. If spin compensation would be dominant mechanism responsible for the low-temperature Kondo-lattice behavior, the $\chi\sim T^{-1/2}$ power law should be observed in the low-temperature limit[37] this is, however, not the case. The susceptibility χ under zero field cooling is not linear with $T^{-1/2}$ either for Fe_2VGa or for small x. From our band-structure calculations results that the compound without AS defects may have a very small (*intrinsic*) susceptibility of $\sim 6\times 10^{-6}$ emu/mol. The underscreened AS defects then add a contribution to the susceptibility that can be considered *extrinsic*. Therefore, an analysis of χ at low temperatures would not show the expected $\chi(T)\sim T^{-1/2}$ Kondo-like behavior for $x<0.2$, since χ is dominated by the undercompensated Kondo effect. With increasing x, the number of carriers increases too, that leads to much better screening of the magnetic moments. Thus $\chi(T)$ shows $T^{-1/2}$ power law at $T<8$ K for the sample $x=0.4$.

C. Electrical resistivity

The evolution of resistivity ρ with Ti substitution is presented in Fig. 9. The data shown in the figure reveal that the pure sample is very poor conductor with resistivity value at 300 K of 415 $\mu\Omega$ cm. The resistivity is gradually decreasing with Ti doping; for $x>0.05$ $\rho(T)$ shows a typical behavior of metals. The apparent maximum in $\rho(T)$ of Fe_2VGa and $Fe_2V_{0.95}Ti_{0.05}Ga$ can be explain in a few ways: (*i*) it can result from an interplay of the spin-glass-like behavior and Kondo effect,[38,39] (*ii*) the Kondo effect is negligible and the maximum arises due to the combined effect of a modified-phonon contribution $\sim -bT$ and the RKKY spin-flip scattering contribution,[40] (*iii*) a negative temperature coefficient of the resistivity (TCR) $d\rho/dT<0$ usually attributed to the

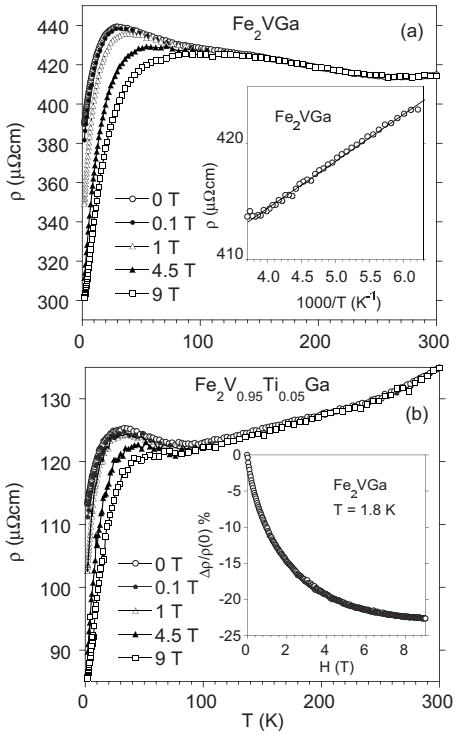

FIG. 10. Temperature dependence of the electrical resistivity of Fe_2VGa [in panel (a)] and $Fe_2V_{0.95}Ti_{0.05}Ga$, (b), at different magnetic fields. The inset (a) displays the resistivity log ρ vs $1/T$. The inset (b) shows magnetoresistance $\Delta\rho/\rho(0)$ vs magnetic field H at 1.8 K indicated in %, $\Delta\rho=\rho(H)-\rho(0)$. The same field dependence of $\Delta\rho/\rho(0)$ is measured for the sample $Fe_2V_{0.95}Ti_{0.05}Ga$ at $T=1.8$ K with the maximal value of $\Delta\rho/\rho(0)\sim 27\%$ at the field $H=9$ T.

strong atomic disorder[41] can be dominated by the inhomogeneous magnetic phase at the temperatures $T<30$ K, finally (*iv*) within the many-electron model,[42] the temperature variation in the quasiparticle structure and the measured quantities such as electrical resistivity, electronic specific heat, etc. can be well described for strongly correlated narrow AS *d*-band interacting via hybridization with a broad band.[19,29]

The role of narrow *d*-AS Fe-bands seems to be important in understanding of the physical properties of the doped Fe_2VGa alloys. Alternatively, as shown in Fig. 9, the resistivity of Fe_2VGa roughly obey the relationship $\rho(T)=a-bT-c/T+e^{\Delta E/T}$, with $\Delta E=1.3$ K. The gap of order 1 K in Fe_2VGa seems rather unphysical here. However, inside very simple approach much more interesting is that the obtained value of $\Delta E\neq 0$, which suggests the presence of narrow pseudogap in the electronic density of states of the system with atomic disorder. Moreover, a broad peak in electrical resistivity coincides with the maximum in ac susceptibility (see Fig. 6), which indicates that the anomaly in $\rho(T)$ can be due to the presence of magnetic defects, such as those measured via field-dependent specific heat (will be discussed). These magnetic defects could lead to negative GMR at $T<\sim 80$ K. The GMR effect is $\sim 25\%$ at $T=1.8$ K in the field of 9 T (see Fig. 10). The same GMR effect was reported very recently for Fe_2VGa (Ref. 24) and discussed in terms of the metal-insulator transition affected by magnetic moments. The model proposed in Ref. 24 bases on the assumption that in the metallic state the magnetic clusters are ordered, whereas weak ferromagnetic coupling among the clusters is broken by thermal fluctuations of the cluster moments in consequence the semiconducting behavior is dominant in the paramagnetic region ($T>T_C$) in the nearly insulating matrix. In the metallic region the ferromagnetic clusters are metallic in their inside, which is well supported by the FP-LAPW calculations in Fig. 2(c), and the electrons can transfer through the nearly insulating matrix [as is shown in Fig. 2(a)] by tunneling between the magnetic clusters. The metallic region can be developed apparently by the magnetic field. In Figs. 9 and 10 the resistivity of Fe_2VGa displays activated behavior between 160 and 260 K; i.e., $\rho(T)\sim e^{\Delta E/k_BT}$ with $\Delta\approx 10$ K. This circumstance resembles to a magnetic semiconductor such as $Ga_{1-x}Mn_xAs$,[43] $In_{1-x}Mn_xAs$,[44] $Ga_{1-x}Mn_xP$,[45] $Ga_{1-x}Mn_xSb$,[46] etc. One of the common important features of these materials is the invariable presence of strong disorder, which plays an essential role in both magnetic and transport properties of the systems with the most prominent effect being the localization of carriers. Although the cluster model[24] explains qualitatively the nature of the maximum in $\rho(T)$ of Fe_2VGa, problems in describing the observation of power-law divergent $C(T)/T$ and $\chi(T)$ with similar exponents in Fe_2VGa and $FeV_{0.95}Ti_{0.05}Ga$ still exists. Our studies of polycrystalline Fe_2VGa and chemically substituted $Fe_2V_{1-x}Ti_xGa$ samples (where $x<0.2$) suggest that a *magnetic ground state* could be responsible for the existence of a Griffiths-McCoy phase. This model predicts power-law behavior of $C(T)/T$ and $\chi(T)$ with the similar power-law exponents.[47] The best fits of the Griffiths-McCoy phase relations $C/T\sim T^{-n}$ and $\chi\sim T^{-n}$ to $C(T)$ and $\chi(T)$ data yield similar values of n ($n=0.34$ and 0.27, respectively) below ~ 5 K. Our data resemble that of Guo *et al.*[48] who claim to have found evidence for Griffiths phases in Co doped FeS_2. In light of the divergent thermodynamic properties at $T\to 0$, Fe_2VGa may be more closely described by model proposed by Manyala *et al.*[49] for *undercompensated Kondo effect* in doping semiconductor FeSi. The magnetotransport data revealed that FeSi doped with Mn is a non-Fermi liquid. It seems that disordered Fe_2VGa doped by Ti belong to the class of *doped small-band gap semiconductors near a metal-insulator transition*, which can also display a non-Fermi liquid state.

As was suggested, the resistivity data presented in Figs. 9 and 10 clearly indicate the importance of magnetic scattering on the carrier transport. The number of carriers is comparable to the number of magnetic defects. The colossal negative magnetoresistance (MR) clearly points this out. In addition, the sharpness of the MR at low fields also indicates that the carriers are in magnetically ordered compound, rather than a paramagnetic compound. In Fig. 9 the low T decrease in the resistivity is clearly indicating a decreases magnetic scattering as the compound orders magnetically below ~ 20 K [see Fig. 7(c)]. This is in good reference to the susceptibility data of Fig. 6(a). The susceptibility saturates at the same temperature where the resistivity decreases. The reason for this decrease and the negative magnetoresistance is the small density of electrical carriers, which are scattered by the magnetic moments. Either a field or an ordering of magnetic

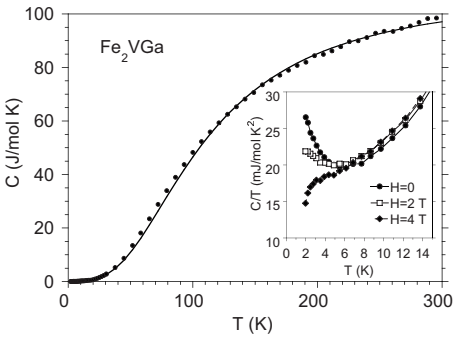

FIG. 11. Temperature dependence of the specific heat of Fe_2VGa. The solid line is a fit discussed in the text. The inset presents the low-temperature data in the form $C(T)/T$ vs T at the magnetic fields $H=0$, 2, and 4 T.

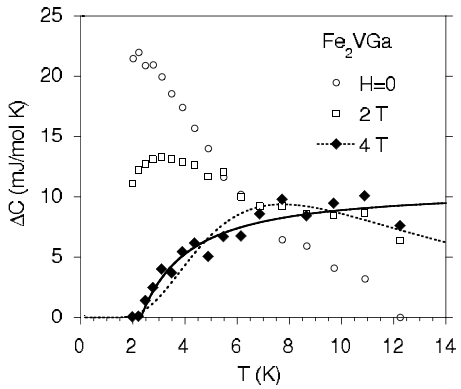

FIG. 12. Temperature dependence of ΔC vs T in magnetic fields of 0, 2 and 4 T. The dotted curve is a fit of a two-level Schottky-like function $C_{Sh}=Nk_B(\epsilon/T)^2e^{\epsilon/T}/(1+e^{\epsilon/T})^2$ to the ΔC data. In the plot $\Delta C=C(T)-(\gamma_0 T+\beta T^3)$, where γ_0 and β are obtained from the linear dependence of C/T vs T^2. The continuous line is a plot of multilevel Schottky function $\Delta C=N_{\mathrm{Fe}}k_B[\frac{x^2e^x}{(e^x-1)^2}-(2J+1)^2\frac{x^2e^{(2J+1)x}}{(e^{(2J+1)x}-1)^2}]$.

moments can remove this scattering resulting in a substantial decrease in the resistivity.

The conclusion from all the thermodynamic electric resistivity and magnetic measurements is that there are residual, unscreened spins either in disordered Fe_2VGa or Fe_2VGa doped by Ti. The Kondo coupling between the low density of carriers and the magnetic moments is not sufficient to screen the moments, which is suggested by the susceptibility. The mechanism underlying the non-Fermi liquid behavior seems to be similar to that proposed very recently for an undercompensated Kondo problem in FeSi:Mn,[49] where there are not enough free carriers with spin $S=1/2$, to screen the remaining local moments associated with AS defects. The effect of doping add carriers (see Fig. 1) which results in a much better screening of the magnetic moments. Thus the resistivity decreases substantially because of an increased carrier density and a decreased scattering rate. This conclusion is well supported by the band-structure calculations, which show increasing of DOS at the Fermi level vs Ti doping. The inset to Fig. 9 indicates a Fermi liquid ground state that is not observed for Fe_2VGa and $Fe_2V_{0.95}Ti_{0.05}Ga$.

The resistivity of Fe_2VGa slightly deviates from activated behavior at $T>\sim 260$ K, which means that the electron-phonon interaction dominates. This deviation is more distinct for $FeV_{0.95}Ti_{0.05}Ga$ at $T>80$ K, whereas the alloys $x=0.2$ and 0.4 displays the metallic character in $\rho(T)$ curves.

D. Specific heat

The resistivity data reveal an importance of magnetic scattering on the carrier transport in Fe_2VGa. The enormous negative magnetoresistance clearly points this out. The Arrott analysis has confirmed the magnetic clusters at lower temperatures which are forming without a global ordering. If this interpretation is correct one would expect a linear-in-T contribution to the specific heat and a Schottky-like peak in $C(T)/T$ at the magnetic fields and low temperatures.

Figure 11 displays temperature dependence of the specific heat of Fe_2VGa measured in zero magnetic field. In temperature region $T>70$ K $C(T)$ can be described by the equation: $C(T)=\gamma T+n\times 9R(\frac{T}{\Theta_D})^3\int_0^{\Theta_D/T}\frac{x^4e^x}{(e^x-1)^2}dx$, in which the first term is the electron specific heat $C_{el}(T)=\gamma T$, while the second one represents the phonon contribution (full Debye expression) characterized by the Debye temperature θ_D, n is the number of atoms per formula unit. The solid line in Fig. 11 presents temperature variation in the calculated specific heat with the parameters $\gamma=27$ mJ/mol K^2, $n=4$, and $\theta_D=433$ K. The specific-heat $C(T)$ data do not show any feature characteristic of the magnetic phase transition for ferromagnetic state, however, the ΔC defined as the measured specific heat subtracted by the calculated C_{el} and phonon contributions has a broad peak with maximum in ΔC of ~ 2.5 J/mol K^2 at the temperature of 70 K, which could be attributed to magnetic inhomogeneous state resulting from the presence of magnetic defects.

The results of specific-heat measurements performed in applied fields 0, 2, and 4 T are shown in the inset of Fig. 12 as C/T vs T. The specific-heat data follow the relationship $C(T)=\gamma_0 T+\beta T^3$. We have fit the data between 8 and 20 K to $C/T=\gamma_0+\beta T^2$ (the fit is not shown in the figure) with $\gamma_0=15.5$ mJ/mol K^2 and $\beta=0.0653$ mJ/mol K^4. In the low-temperature limit, the Debye temperature θ_D obtained from $\beta=\frac{12\pi^4}{5}\frac{nR}{\Theta_D^3}$ is 492 K. A very similar parameters were obtained recently[50] from the specific-heat data for Fe_2VGa. The low-T upturn in C/T at $H=0$ was interpreted as result of Schottky-like anomalies due to magnetic defects.[8,50] Namely, assuming that the specific heat is a sum, $\Delta C+\gamma_0 T+\beta T^3$, and using the γ_0 and β parameters extracted above, it is possible to fit the ΔC data at $H=4$ T to a two-level Schottky function $C_{Sh}=N_{\mathrm{Fe}}k_B(\epsilon/T)^2e^{\epsilon/T}/(1+e^{\epsilon/T})^2$, with $\epsilon=18.7$ K. In Fig. 12 the line is the best fit of expression to the experimental data. However, similar field dependence of $C(T)/T$ is observed for several f-electron heavy fermion materials. While the low-T upturn in C/T could be associated with narrow d-band of AS Fe defects, the γ value should be renormalized by the large effective mass m^* and the enhanced DOS at the Fermi level. For these type of Fe-Heusler alloys the effective mass is even $40\times m_0$,[16] also FP-LAPW gives for the defected $[Fe_{14}V_2^{AS}][V_6Fe_2^{AS}]Ga_8$ the DOS at ϵ_F of ~ 5.5 eV^{-1} f.u.$^{-1}$.

In Fig. 12 the specific-heat data appear to indicate the presence of a large number of magnetic moments, which are

not interacting with their neighbor. A simple fit of Schottky function to the ΔC data at $H=4$ T (dotted curve) gives a large number of $\sim 7\times 10^{16}$ cm^{-3} of Schottky centers, thus the increased $C(T)/T$ at zero field and at low temperatures. We also fit ΔC for a field 4 T to the multilevel Schottky function:[51] $\Delta C = N_{\mathrm{Fe}} k_B \left[\frac{x^2 e^x}{(e^x-1)^2} - (2J+1)^2 \frac{x^2 e^{(2J+1)x}}{(e^{(2J+1)x}-1)^2}\right]$, where $x = g\mu_B H/k_B T$. The fit with $g=1.93$, $J=3/2$, and $N_{\mathrm{Fe}} = \sim 4 \times 10^{16}$ cm^{-3} is plotted in Fig. 12 as continuous curve. A magnetic field shifts the ΔC contribution to the specific heat to higher temperatures as shown in Fig. 12, resulting in a Schottky-like anomaly in $C(T)/T$ shown in Fig. 11. This behavior is consistent with a large scattering potential for the electrical carriers from fluctuating magnetic moments. The observation, that ΔC maximum decreases with increasing applied field and shifts towards higher temperatures is characteristic for canonical spin glasses.[52]

V. SUMMARY

Fe_2VAl and Fe_2TiSn Heusler alloys have recently been discussed as possible *d*-electron heavy fermions, where the resistivity displays an anomalous temperature dependence, and specific-heat measurements reveal an upturn in $C(T)/T$ resembling that of conventional *f*-electron HF compounds. From the optical conductivity data it has been shown that these both alloys have a deep pseudogap at the Fermi level,[15,16] which is unusual for intermetallic compounds. However, an infrared study have found no characteristic features of the HF state in these alloys, which is in contradiction to the specific-heat $C(T)/T$ data at $T\rightarrow 0$. Alternatively, crystallographic disorder resulting from atomic site exchange between Fe or Ti atoms can lead to clusters, which could explain the low-T physical properties of Fe_2VAl or Fe_2TiSn alloys, respectively. The model which assumes that the physical properties of the nonmagnetic Fe_2VAl or Fe_2TiSn are dominated by atomic Fe defects is generally accepted, while Kondo insulating state seems not to be dominated. However, these Fe antisite defects give rise to the narrow, strongly correlated *d* band, as was shown in Refs. 19 and 31. In this scenario, several low-T properties observed in Fe_2VAl or Fe_2TiSn resemble those in the nonmagnetic narrow-gap semiconductor FeSi, known as the *d*-electron Kondo insulator.[53]

Experimental investigations have shown that several properties observed in Fe_2VGa, e.g., low-T upturn in C/T, the pseudogap at ϵ_F in the DOS, and the narrow *d* band at ϵ_F resulting from atomic disorder, resemble those characteristic of Fe_2VAl and Fe_2TiSn. The electronic structure calculations have shown that Fe_2VGa is semimetallic and nonmagnetic. The FP LAPW method proved that Fe defects also form in the supercell $[Fe_{14}V_2^{AS}][V_6Fe_2^{AS}]Ga_8$ the narrow and correlated *d*-bands at the Fermi level, however, the Fe_{AS} defects are calculated as nonmagnetic in contrast to the remaining systems (Fe_2TiSn and Fe_2VAl) discussed here. The frequency dependence of χ indicates, however, formation of the spin-glass-type behavior due to the Fe-defects different than that, considered for the supercell $[Fe_{14}V_2^{AS}][V_6Fe_2^{AS}]Ga_8$. It is possible to generate magnetic Fe_{AS} clusters in the disordered system $Fe_{3-x}V_xGa$. The band-structure calculations for $x=0.5-0.94$ confirmed the conclusions drawn from experiments about the existence of magnetic clusters.[30] For small concentrations of Fe_{AS} atoms calculations have shown that AS impurities together with eight surrounding Fe atoms form the magnetic clusters. The magnetic moment of the Fe-AS atoms is large ($\sim 2.7\ \mu_B$).[30] Therefore, the magnetic properties of Fe_2VGa alloy can be interpreted as follows: the stoichiometric intermetallic compound is nonmagnetic, but contain Fe defects with magnetic moments in the off stoichiometric volume fractions of the sample. The Fe-defects can give contribution to spin glass-like (superparamagnetic) behavior leading to false heavy fermion behavior. The magnetic and resistivity data presented indicate that there is a tremendous importance of magnetic scattering on the carrier transport. Our data suggest that Fe_2VGa is the system with undercompensated Kondo effect, resulting from atomic disorder and formation of a pseudogap at the Fermi level. It is clear then that the Kondo coupling between the low density of carriers and the magnetic moments is not sufficient to screen the moments. Therefore, the low-temperature dependence in the resistivity is indicating decreased magnetic scattering due to the magnetic order observed below ~ 20 K. Magnetic field removes the scattering potential producing a large negative magnetoresistance. The specific-heat data indicate the presence of a large number of noninteracting and partially screened magnetic moments which gives rise to the low-T upturn in $C(T)/T$ at $H=0$. The number of these moments is comparable to the number of carriers.

The effect of Ti doping leads to increasing of the density of carriers, in effect the $Fe_2V_{1-x}Ti_xGa$ alloys with $x>0.2$ are metallic, with much better Kondo screening. Our measurements suggest that the pseudogap in Fe_2VGa is rapidly suppressed even by a small amount of Ti, suggesting the importance of changing the number of valence electrons. A similar effect of increasing the number of conduction electrons on the hybridization gap was recently observed in the Kondo insulator CeRhSb, when Sb is substituted by Sn.[54] In the case of Fe_2VGa the gap is, however, strongly destroyed by magnetic correlations due to the presence of magnetic Fe defects, therefore the system $Fe_2V_{1-x}Ti_xGa$ of alloys easily evolves from semimetallic to metallic character.

ACKNOWLEDGMENTS

The authors thank the Polish Ministry of Science and Education for support from Project No. N N202 032137.

[1] P. S. Riseborough, Adv. Phys. **49**, 257 (2000).
[2] P. A. Lee, T. M. Rice, J. W. Serene, L. J. Sham, and J. W. Wilkins, Comments Condens. Matter Phys. **12**, 99 (1986).
[3] V. Jaccarino, G. K. Wertheim, J. H. Wernick, L. R. Walker, and S. Arajs, Phys. Rev. **160**, 476 (1967).
[4] G. Aeppli and Z. Fisk, Comments Condens. Matter Phys. **16**, 155 (1992).
[5] Y. Nishino, M. Kato, S. Asano, K. Soda, M. Hayasaki, and U. Mizutani, Phys. Rev. Lett. **79**, 1909 (1997).
[6] A. Ślebarski, M. B. Maple, E. J. Freeman, C. Sirvent, D. Tworuszka, M. Orzechowska, A. Wrona, A. Jezierski, S. Chiuzbaian, and M. Neumann, Phys. Rev. B **62**, 3296 (2000).
[7] Z. Schlesinger, Z. Fisk, H.-T. Zhang, M. B. Maple, J. F. DiTusa, and G. Aeppli, Phys. Rev. Lett. **71**, 1748 (1993).
[8] C. S. Lue, J. H. Ross, Jr., C. F. Chang, and H. D. Yang, Phys. Rev. B **60**, R13941 (1999).
[9] D. J. Singh and I. I. Mazin, Phys. Rev. B **57**, 14352 (1998).
[10] G. Y. Guo, G. A. Button, and Y. Nishino, J. Phys.: Condens. Matter **10**, L119 (1998).
[11] R. Weht and W. E. Pickett, Phys. Rev. B **58**, 6855 (1998).
[12] O. K. Andersen and O. Jepsen, Phys. Rev. Lett. **53**, 2571 (1984); O. K. Andersen, O. Jepsen, and M. Sob, in *Electronic Structure and Its Applications*, edited by M. Yussouff (Springer, Berlin, 1987), p. 2.
[13] Ye Feng, J. Y. Rhee, T. A. Wiener, D. W. Lynch, B. E. Hubbard, A. J. Sievers, D. L. Schlagel, T. A. Lograsso, and L. L. Miller, Phys. Rev. B **63**, 165109 (2001).
[14] M. Weinert and R. E. Watson, Phys. Rev. B **58**, 9732 (1998).
[15] H. Okamura, J. Kawahara, T. Nanba, S. Kimura, K. Soda, U. Mizutani, Y. Nishino, M. Kato, I. Shimoyama, H. Miura, K. Fukui, K. Nakagawa, H. Nakagawa, and T. Kinoshita, Phys. Rev. Lett. **84**, 3674 (2000).
[16] S. V. Dordevic, D. N. Basov, A. Ślebarski, M. B. Maple, and L. Degiorgi, Phys. Rev. B **66**, 075122 (2002).
[17] K. I. Wysokiński, Phys. Rev. B **60**, 16376 (1999).
[18] J. Deniszczyk and W. Borgieł, Acta Phys. Pol. B **34**, 1257 (2003).
[19] A. Ślebarski, J. Deniszczyk, W. Borgieł, A. Jezierski, M. Swatek, A. Winiarska, M. B. Maple, and W. M. Yuhasz, Phys. Rev. B **69**, 155118 (2004).
[20] I. Galanakis, P. H. Dederichs, and N. Papanikolaou, Phys. Rev. B **66**, 174429 (2002).
[21] A. Bansil, S. Kaprzyk, P. E. Mijnarends, and J. Toboła, Phys. Rev. B **60**, 13396 (1999).
[22] C. S. Lue and J. H. Ross, Jr., Phys. Rev. B **63**, 054420 (2001).
[23] N. Kawamiya, Y. Nishino, M. Matsuo, and S. Asano, Phys. Rev. B **44**, 12406 (1991).
[24] K. Endo, H. Matsuda, K. Ooiwa, M. Iijima, K. Ito, T. Goto, and A. Ono, J. Phys. Soc. Jpn. **66**, 1257 (1997).
[25] H. Ohno, Science **281**, 951 (1998).
[26] Y. Baer, G. Busch, and P. Cohn, Rev. Sci. Instrum. **46**, 466 (1975).
[27] P. Blaha, K. Schwarz, G. K. H. Madsen, D. Kvasnicka, and J. Luitz, *WIEN2k, An Augmented Plane Wave + Local Orbitals Program for Calculating Crystal Properties* (Karlheinz Schwarz, Techn. Universität Wien, Austria, 2001).
[28] J. P. Perdew, K. Burke, and M. Ernzerhof, Phys. Rev. Lett. **77**, 3865 (1996).
[29] J. Deniszczyk and W. Borgieł, Acta Phys. Pol. A **98**, 551 (2000).
[30] J. Deniszczyk, Acta Phys. Pol. B **32**, 529 (2001).
[31] A. Ślebarski, J. Goraus, J. Deniszczyk, and Ł. Skoczeń, J. Phys.: Condens. Matter **18**, 10319 (2006).
[32] S. Tougaard and P. Sigmund, Phys. Rev. B **25**, 4452 (1982).
[33] J. J. Yeh and I. Lindau, At. Data Nucl. Data Tables **32**, 1 (1985).
[34] F. D. Murnaghan, Proc. Natl. Acad. Sci. U.S.A. **30**, 244 (1944).
[35] C. M. Hurd, Contemp. Phys. **23**, 469 (1982).
[36] A. C. Hewson, *The Kondo Problem to Heavy Fermions* (Cambridge University Press, Cambridge, 1993).
[37] P. W. Anderson, Phys. Rev. **164**, 352 (1967).
[38] U. Larsen, Phys. Rev. B **14**, 4356 (1976).
[39] K. H. Fischer, Z. Phys. B **42**, 27 (1981).
[40] Fu-sui Liu, W. A. Roshen, and J. Ruvalds, Phys. Rev. B **36**, 492 (1987).
[41] J. H. Mooij, Phys. Status Solidi A **17**, 521 (1973).
[42] S. H. Liu, Physica B **240**, 49 (1997).
[43] H. Ohno, A. Shen, F. Matsukura, A. Oliwa, A. Endo, S. Katsumoto, and Y. Iye, Appl. Phys. Lett. **69**, 363 (1996).
[44] H. Ohno, H. Munekata, T. Penney, S. von Molnár, and L. L. Chang, Phys. Rev. Lett. **68**, 2664 (1992).
[45] N. Theodoropoulou, A. F. Hebard, M. E. Overberg, C. R. Abernathy, S. J. Pearton, S. N. G. Chu, and R. G. Wilson, Phys. Rev. Lett. **89**, 107203 (2002).
[46] X. Chen, M. Na, M. Cheon, S. Wang, H. Luo, B. D. McCombe, X. Liu, Y. Sasaki, T. Wojtowicz, J. K. Furdyna, S. J. Patashnik, and P. Schiffer, Appl. Phys. Lett. **81**, 511 (2002).
[47] R. B. Griffiths, Phys. Rev. Lett. **23**, 17 (1969); A. H. Castro Neto, G. Castilla, and B. A. Jones, *ibid.* **81**, 3531 (1998).
[48] S. Guo, D. P. Young, R. T. Macaluso, D. A. Browne, N. L. Henderson, J. Y. Chan, L. L. Henry, and J. F. DiTusa, Phys. Rev. Lett. **100**, 017209 (2008).
[49] N. Manyala, J. F. DiTusa, G. Aeppli, and A. P. Ramirez, Nature (London) **454**, 976 (2008).
[50] C. S. Lue, H. D. Yang, and Y. K. Kuo, Chin. J. Phys. (Taipei) **43**, 775 (2005).
[51] R. L. Falge, Jr. and N. M. Wolcott, J. Low Temp. Phys. **5**, 617 (1971).
[52] J. A. Mydosh, *Spin Glasses, an Experimental Introduction* (Taylor and Francis, London, 1993).
[53] The specific heat $C(T)/T$ of Fe_2TiSn exhibits a pronounced maximum at $\sim$1.1 K which was interpreted as a result of Schottky anomaly due to magnetic excitation (Ref. 6). The possible reason of this maximum would also be a formation of the Kondo semimetallic state.
[54] A. Ślebarski and J. Spałek, Phys. Rev. Lett. **95**, 046402 (2005).